Assessment of high-efficacy agonism in synthetic cannabinoid receptor agonists containing l-*tert*-leucinate

Christopher Lucaj, Charlotte Pitha, Jordan Davis, Hideaki Yano*

Department of Pharmaceutical Sciences, School of Pharmacy and Pharmaceutical Sciences, Bouvé College of Health Sciences, Center for Drug Discovery, Northeastern University, Boston, Massachusetts 02115, United States

*h.yano@northeastern.edu

Abstract

Synthetic cannabinoid receptor agonists (SCRAs) represent a class of new psychoactive substances that pose great health risks attributed to their wide-ranging and severe adverse effects. Recent evidence has shown that SCRAs with key moieties can confer superagonism, yet this phenomenon is still not well understood. In this study, we developed a structure-activity relationship (SAR) for SCRA superagonism by comparing eight compounds differing by their head moiety (l-valinate vs. l-*tert*-leucinate), core moiety (indole vs. indazole), and tail moiety (5-fluoropentyl vs. 4-fluorobenzyl) through different modes of bioluminescence resonance energy transfer (BRET). We found that l-*tert*-leucinate head moiety and indazole core moiety conferred superagonism across multiple $G\alpha_{i/o}$ proteins and β-arrestin 2. Finally, after generating CB1R mutant constructs, we found that transmembrane 2 (TM2) interactions to the head moiety of tested SCRAs at F170, F177, and H178 are key to eliciting activity.

Introduction

The severe adverse effects observed with SCRA use are distinct from those of delta-9-tetrahydrocannabinol (THC), the active compound found in *Cannabis sativa* [1-4]. Due to their chemical structures, specifically aminoalkyl-heterocycle SCRAs, countless drugs can be illicitly made through iterative design, resulting in greatly increased efficacy and potency. Use of one of these SCRAs, MMB-FUBINACA, was responsible for a well-publicized case of SCRA intoxication that occurred in 2016 when thirty-three people exhibiting “zombie-like” cataleptic behavior [5]. In a separate clinical case, patients experienced extreme agitation, aggressiveness, and seizures after using another SCRA

ADB-PINACA [3]. Finally, SCRA overdose can be lethal, which is not reported with cannabis use [6, 7].

SCRAs are designed to target the cannabinoid type 1 receptor (CB1R), a highly expressed G-protein coupled receptor (GPCR) in the brain and CNS [1, 8]. CB1R plays a crucial role in downregulating neurotransmitter release, primarily through $G\alpha_{i/o}$ signaling pathways initiated by retrograde signaling at synaptic terminals [9, 10]. Upon G-protein activation, voltage-gated Ca^{2+} channels are inhibited and G-protein inward rectifying K^+ channels are activated, resulting in pre-synaptic hyperpolarization [9, 11]. Peripherally, the receptor also plays an important role in cardiovascular function as well as energy metabolism [12-14]. CB1R expression and function in multiple systems are complemented by the differential expression of the $G\alpha_{i/o}$ protein subfamily, consisting of ubiquitously ($G\alpha_{i1}$, $G\alpha_{i2}$, $G\alpha_{i3}$) and neuronally ($G\alpha_{oA}$, $G\alpha_{oB}$, $G\alpha_{z}$) expressed inhibitory G-proteins [15-18]. Pharmacological studies have characterized a number of SCRAs based on CB1R-mediated cAMP inhibition as well as β-arrestin internalization[19-22]. SCRA-induced G-protein signaling within the subfamily of $G\alpha_{i/o}$ proteins, however, has only been investigated very recently[21, 23, 24]. Though these studies found SCRAs to show little functional selectivity or bias, a thorough comparison of moieties among structural analogs has not been attempted by using rigorous proximity assay approaches.

Understanding SCRA pharmacology has been a challenge mainly addressed through functional assays to assess potency and efficacy. Indeed, structure-activity relationships of these chemical structures, composed of three key moieties (head, core, and tail), have led to a characterization of SCRAs as “high efficacy” agonists [5, 7, 19, 20]. However, signal amplification in assays that measure activity downstream of receptor-transducer interactions can changes in efficacy, yet report increased potency [25]. Recently, we investigated the SAR between two compounds, 5F-MMB-PICA (M-PC) and 5F-MDMB-PICA (D-PC), that differed in a single methyl group in the “head” moiety [26]. D-PC, with an l-*tert*-leucinate head moiety, was shown to act as a “superagonist”, an agonist that has greater efficacy than that of the endogenous ligand, while M-PC acted as a full agonist[25, 26]. Notably, molecular dynamics simulations between these drugs revealed different levels of interaction with key residues in the extracellular TM2 domain, a region recently reported to be critical in activation of CB1R [26-29]. Although we found a SCRA that elicits superagonism, an understanding of what drives CB1R superagonism is still limited.

In the current study, we further explore differences in SCRA moieties to uncover CB1R superagonism based on differences in “head,” “core,” and “tail” moieties. With a panel of eight compounds we use different modes of bioluminescence resonance energy transfer (BRET) to assess the efficacy, bias, and functional selectivity of these compounds. Finally, we developed CB1R mutants in key TM2 residues to reveal key interactions with the head moiety l-*tert*-leucinate.

Materials and Methods

Mammalian Cell Culture All *in vitro* assays are performed in human embryonic kidney 293 T (HEK-293T) cells cultured in Dulbecco's Modified Eagle Medium (DMEM) supplemented with 10% fetal bovine serum (FBS), 1% penicillin/streptomycin, and 2 mM L-glutamine and incubated at 37°C and 5% CO_2. HEK-293T cells are cultured in 10-cm plates at a high cell density of 375,000 cells/ml (3 x 10^6 cells/8 ml) twenty-four hours prior to transfection. Cells are maintained using aseptic technique and are used in pharmacological assays within 5-30 passages.

Compounds & Plasmid Constructs All CB1R ligands used in this study are purchased or acquired from Cayman Chemical (Ann Arbor, Michigan) or NIDA Drug Supply Program (Rockville, Maryland). The ligands are dissolved in DMSO to a stock concentration of 10 mM. All DNA constructs are generated in pcDNA3 plasmid vectors. Alanine substitutions of *CNR1*-containing plasmid constructs were generated using the Quickchange Site-Directed Mutagenesis Kit (Agilent) and the following primers:
F170A forward primer 5' – TGGGGAGTGTCATTGCTGTCTACAGCTTCAT – 3',
reverse primer 5' – ATGAAGCTGTAGACAGCAATGACACTCCCCA – 3';
S173A forward primer 5' – TCATTTTTGTCTACGCCTTCATTGACTTCCA – 3',
reverse primer 5' – TGGAAGTCAATGAAGGCGTAGACAAAAATGA 3';
F174A forward primer 5' – ACAGCTTCATTGACGCCCACGTGTTCCACC – 3',
reverse primer 5' – GGTGGAACACGTGGGCGTCAATGAAGCTGT – 3';
F177A forward primer 5' – TTTTTGTCTACAGCGCCATTGACTTCCACG – 3',
reverse primer 5' – CGTGGAAGTCAATGGCGCTGTAGACAAAAA – 3';
H178A forward primer 5' – GCTTCATTGACTTCGCCGTGTTCCACCGCA – 3',
reverse primer 5' – TGCGGTGGAACACGGCGAAGTCAATGAAGC – 3'.

Bioluminescence Resonance Energy Transfer (BRET) receptor function assays BRET assays described below contain variations in DNA constructs transfected and in method of experimentation. Consistent with all experiments is a pre-incubation of 5-15 µg DNA (per 10-cm plate, DNA amounts vary by experiment) with 30 µg/cell plate linear polyethyleneimine (PEI) in serum-free DMEM twenty minutes before addition to cells. After overnight treatment, media is fully replaced with fresh, supplemented DMEM. After 48 hours of transfection, cells are washed with phosphate-buffered saline (PBS), harvested, and resuspended in PBS containing 0.1% glucose and 200 µM sodium bisulfite, which serves as a drug stabilizer. Cells are evenly distributed amongst wells in white flat-bottom 96 well plates. On the day of experiment, serially diluted drugs are transferred to cells three minutes after 5 µM coelenterazine H incubation. Luminescence and fluorescence values are recorded 10 minutes after drug treatment in a PheraStar FSX plate reader (bioluminescence at 480 nm, fluorescence at 530 nm). BRET ratio is

calculated based on the measurement of fluorescence divided by that of luminescence. BRET ratios are then normalized to the basal BRET ratio calculated by the non-linear regression generated by GraphPad Prism 10.

G-protein/β-arrestin engagement – Plasmid DNA in engagement BRET assays have been reported [26] as follows: 0.5 µg CB1R tagged with *Renilla* luciferase 8 (CB1R-RLuc), 5 µg $G\alpha_{i1}$ tagged with Venus ($G\alpha_{i1}V$), and 4 µg of both $G\beta_1$ and $G\gamma_2$. For β-arrestin engagement, 6 µg of β-arrestin-2 tagged with Venus (βArr2V) and 5 µg of G-protein coupled receptor kinase 2 (GRK2) are used. They have been reported previously.

G-protein activation – Plasmid DNA in activation BRET assays have been reported [30, 31] as follows: 3.5 µg CB1R untagged, 0.5 µg Gα tagged with *Renilla* luciferase 8 ($G\alpha_{i1}$-RLuc, $G\alpha_{i2}$-RLuc, $G\alpha_{i3}$-RLuc, $G\alpha_{oA}$-RLuc, $G\alpha_{oB}$-RLuc, or $G\alpha_z$-RLuc), 4 µg of $G\beta_1$ and 5 µg of $G\gamma_2$ tagged with Venus ($G\gamma_2V$).

Data Analysis. All data was processed and analyzed in GraphPad Prism 10 (San Diego, California). Data points were transformed to individual BRET ratio values and further normalized to the minimal and maximal responses by CP55,940 at 10 min as 0% and 100% respectively within each respective transducer. E_{max} and pEC_{50} parameters were obtained from the non-linear fit of normalized transformed data and multi-comparison data analyses at the 10 min time point were conducted. Based on the extrapolated curves, E_{max} and pEC_{50} are determined. E_{max} on a non-plateaued curve and pEC_{50} less than 5 are still reported in the tables. In those cases, E_{max} is reported as the efficacy at the highest concentration observed (10 µM). To evaluate whether SCRAs exhibited G protein subunit signaling bias, bias factors were calculated as reported previously [32]. This method yields bias factors similar to the operational model. Briefly, $\Delta\log(E_{max}/EC_{50})$ value for each transducer was calculated by subtracting the $\log(E_{max}/EC_{50})$ value of the agonist by that of the reference compound. $\Delta\Delta\log(E_{max}/EC_{50})$ is determined by subtraction of $\Delta\log(E_{max}/EC_{50})$ between two transducers. The comparison between the two transducers shows the bias direction of a certain ligand towards one of the two transducers. Throughout the experiments, a triplicate of at least four independent experiments was performed per each condition. Statistical grouped analyses on E_{max} and pEC_{50} were conducted using one-way ANOVA with a post-hoc Dunnett test for multiple comparisons.

Results and Discussion

L-*tert*-leucinate head moiety leads to high efficacy in SCRA derivatives.

After recently investigating the drastic efficacy differences between l-valinate and l-*tert*-leucinate (*i.e.*, MMB- and MDMB-) head moieties of 5-fluoropenylindoles, we expanded our investigation on core and tail moieties in combination to the head moiety[26]. Clinical studies have reported on the severe impact of indazole-based SCRA abuse, including

death from overdose [3, 5, 33, 34]. Furthermore, original derivatives patented by Pfizer, as well as the drug responsible for the 2016 Brooklyn outbreak, carried a 4-fluorobenzyl tail moiety[5]. Therefore, we selected 5F-MMB-PICA (M-PC), 5F-MDMB-PICA (D-PC), 5F-MMB-PINACA (M-PN), 5F-MDMB-PINACA (D-PN), MMB-FUBICA (M-FC), MDMB-FUBICA (D-FC), MMB-FUBINACA (M-FN), MDMB-FUBINACA (D-FN) for our study panel to develop a SAR of these moieties for CB1R superagonism (Fig. 1).

We began our study with measuring the engagement of $G\alpha_{i1}$ and β-arrestin-2 to CB1R using an "engagement" mode of BRET where the receptor and Gα-protein or β-arrestin are tagged with luciferase and fluorescent proteins, respectively (Fig. 2A, 1D). M-PC displayed full agonism and D-PC displayed superagonism accompanied by higher potency in $G\alpha_{i1}$ engagement (Fig. 2B) as previously reported [26]. We see this similar, respective separation in efficacy and potency for the 4-fluorobenzyl analogues M-FC and D-FC (Fig. 2C). Interestingly, the difference in efficacy between MMB- and MDMB-compounds is negligible amongst indazole SCRAs (*i.e.*, M-PN, D-PN, M-FN, D-FN), as all confer superagonism, although there is still a noticeable potency shift for the MDMB-series (Fig. 2B-C, Table 1). Within β-arrestin-2, seven of the eight SCRAs are more efficacious than the reference compound CP55940, with only M-FC acting as a full agonist (2E-F, Table 1). Although an insignificant difference for $G\alpha_{i1}$ engagement, the 5-fluoropentyl SCRAs were all approximately 35-70% greater in efficacy than their 4-fluorobenzyl analogues (2E-F, Table 1).

Previous studies assessed a number of SCRAs used here as "high efficacy" agonists [36, 37]. By using the BRET "engagement" mode, we better address issues associated with signal amplification and receptor reserves, which can result in falsely high efficacy and potency activity in downstream functional assays [25, 35], as the engagement mode detect direct coupling between the receptor and transducer. Indazoles, regardless of head or tail moiety within the structure, drastically increases SCRA efficacy and potency, the latter of which has been well reported for indazole SCRA derivatives [20, 21]. The superagonist activity of D-PC, D-PN, and D-FN, in both $G\alpha_{i/o}$ and β-arrestin engagement, may be a determining factor in the severity of the adverse effects, as cannabis use, thus moderate efficacy of THC on CB1R, rarely causes the severe adverse effects and toxicities [7]. The increased efficacy in β-arrestin-2 engagement may be associated with increased tolerance found in SCRA use as β-arrestins mediate CB1R internalization [38, 39]. Indeed, SCRAs have been reported to induce rapid CB1R internalization through β-arrestin [21, 24]. Here, we found that M-FC and D-FC displayed β-arrestin-2 bias, with all the indazole-containing SCRAs leaning towards β-arrestin-2 bias, albeit not below the -1 threshold (Table 1). These findings clearly indicate that high efficacy in β-arrestin may play a role in adverse effects reported in human use.

SCRA superagonism is observed across activation of most $G\alpha_{i/o}$ subtypes.

Numerous studies have reported on SCRA-mediated CB1R activities without identifying the involvement of specific $G\alpha_{i/o}$ subtypes. Concurrently, there are limited findings on SCRA agonism amongst the six main inhibitory G proteins ($G\alpha_{i1}$, $G\alpha_{i2}$, $G\alpha_{i3}$, $G\alpha_{oA}$, $G\alpha_{oB}$, $G\alpha_{z}$). Therefore, we aim to study the extent of SCRA superagonism across the $G\alpha_{i/o}$ subtypes, as well as the contribution of key moieties in the functional selectivity of these SCRAs.

To investigate this, we use an "activation" mode of BRET to measure the G-protein heterotrimer dissociation via untagged CB1R (Fig. 3A). Amongst indole SCRAs, there was a noticeable increase in both efficacy and potency for MDMB series compared to MMB series (Fig. 3B-D), in line with our BRET "engagement" assay results (Fig. 2A-C). Interestingly, M-FC conferred partial agonism in all $G\alpha_{i/o}$ subtypes except for $G\alpha_{i2}$. There is an efficacy difference between MMB- and MDMB- indazoles in the Gαi subtypes with little change in potency (Fig. 3B-D). Indeed, for $G\alpha_{i1}$ and $G\alpha_{i2}$ activation, M-PN and M-FN conferred partial agonism (Fig. 3B-C). In $G\alpha_{oA}$, we found that M-PN was the single instance of an MMB- compound displaying noticeably greater efficacy than its MDMB-analogue (Fig. 3E). Although most of the compounds were more potent than the reference agonist CP55940 for $G\alpha_{oB}$ and $G\alpha_{z}$ activation, none had been more than 120% effective (Fig. 3F-G, Table 2).

We further analyzed $G\alpha_{i/o}$ subtype activation by estimating each compound's functional selectivity by calculating bias factors. Here, we determined the $\Delta\log(E_{max}/EC_{50})$ of each SCRA to compare two different transducers then taking the difference between the Δ values of a particular SCRA and the reference agonist CP55940, obtaining $\Delta\Delta\log(E_{max}/EC_{50})$ (Table 3). Here we found that none of the compounds had a ΔΔlog value outside the range of -1 to 1, thus suggesting the tested SCRAs are not biased towards any specific pathway.

Through BRET activation, we determined that the panel of tested SCRAs displays superagonism across $G\alpha_{i/o}$ subtypes. This finding is crucial as most previous reports have not focused on SCRA characterization of all $G\alpha_{i/o}$ subtypes and the diverse $G\alpha_{i/o}$ subtype expression in different organs and cell-types may lay background for biased pharmacology. Indeed, the $G\alpha_{i}$ are ubiquitously expressed throughout the body and are the dominant $G\alpha_{i/o}$ subtypes in the periphery, as the $G\alpha_{o}$ proteins and $G\alpha_{z}$ are the dominant proteins in the CNS. SCRA-induced superagonism across these subtypes may suggest a connection to the wide-range of adverse effects from SCRA use, even though these compounds were found to be relatively balanced. Further processing of ΔΔlog values to yield ΔΔΔlog and cross-comparison within the pairs of a differing core, head or tail moiety did not identify any significant bias beyond the -1 or 1 threshold (data not shown). Clinically reported SCRAs have also been found relatively balanced using similar *in vitro* assays [21-23]. Since there are a multitude of combinatorial diversity among different head, core and tail moieties for SCRAs, characterization of signaling bias

remains to be explored and incomplete at present. Here though, we have determined that across $G\alpha_{i/o}$ subtypes, the panel of paired SCRA analogs at head, core and tail moieties display CB1R superagonism.

F170, F177, and H178 are key residues in SCRA activation, not exclusive to l-*tert*-leucinate.

After having established the consistent increase in efficacy and potency for l-*tert*-leucinate (*i.e.*, MDMB-) containing SCRAs, we investigated residues within the binding pocket essential for conferring superagonism. Recent research has found that extracellular transmembrane domain 2 (TM2) residues are implicated in CB1R activation as they rotate inwards in the presence of a full agonist [27, 28]. Indeed, we previously reported on the conformational stability of TM2 being associated with 5F-MDMB-PICA superagonism [26]. Here, we expanded our investigation by generating alanine substitutions along the TM2 residues in order to isolate the essential residues implicated in CB1R superagonism.

We conducted $G\alpha_{oA}$ "activation" BRET with single-point alanine-substituted CB1R constructs at F170, S173, F174, F177, and H178, intracellular to extracellular on TM2, using CP55940 and two representative SCRAs M-PC, and D-PC (Fig. 4A). By establishing the E_{max} of CP55940 for the wildtype CB1R as 100% efficacy, mutational effects were studied on the SCRAs. The F170A substitution reduced the efficacy of all three agonists to a weak partial level (Fig. 4C). The S173A substitution produced no meaningful difference in efficacy and potency than the wildtype (Fig. 4D). Interestingly, the F174A mutation lowered potency by 10-fold or more for all three agonists, but only a decrease in efficacy for M-PC and CP55940 (Fig. 4E). Similarly to F170A, the F177A mutation reduced the efficacy of all three agonists to a weak partial level (Fig. 4F). Finally, the H178A mutation yielded no efficacy in concentration response (Fig. 4G).

In this mutational study, we investigated the TM2 residues implicated in SCRA-mediated CB1R superagonism. Recent reports have indicated that H178 is implicated in the activation of the CB1R [27, 29]. We confirmed that to be the case as the alanine substitution abrogated any response to the three agonists tested. This phenomenon implicates the ring structure and/or positive charge of histidine as essential in CB1R engagement to an agonist in general, beyond head moiety interaction in the aminoalkylindole agonists, warranting further investigation. F170A and F177A reduced efficacy and potency drastically for the three agonists tested, implicating these residues are also essential for agonist activation in general. F174 potentially may stabilize the head moiety of SCRA, based on the cryo-EM structure. Our results show that it is not impactful towards its efficacy, albeit the reduced potency for all three agonists. Similarly, we expected the head moiety of M-PC and D-PC to fully interact with S173 and the S173A mutation to lower their efficacy [26]. On the contrary, interestingly, it substantially increased the efficacy for CP55940 and M-PC, indicating S173 may play a role in

enhanced efficacy. Further investigation on these and other interacting residues beyond TM2 will provide more insight into SCRA superagonism and key interactions with SCRA core and tail moieties as well.

Conclusion

The iterative design of SCRAs in their modular components has led to an explosive number of substances, many manifested toxicities. In this study, we attempted to understand the involvement of TM2 in a SAR for SCRA-induced CB1R superagonism. Using structural pairwise comparison within head, core, and tail moieties, we detailed superagonism conferred by the l-*tert*-leucinate head moiety. We found that SCRAs, depending on their key moieties, can elicit superagonism through multiple $G\alpha_{i/o}$ subtypes and β-arrestin, and that F170, F177, and H178 in TM2 are implicated in conferring such drug action. This pairwise comparison approach within ligand structure in conjunction with extensive transducer analysis may be useful for revealing specific activation profiles in the future SAR studies for novel SCRAs.

Acknowledgements The work is supported by the Brain & Behavior Research Foundation Young Investigator Grant (H.Y.) and by the National Institute on Drug Abuse (T32DA055553 to C.L.)

Author Contributions C.L., H.Y. designed the experiments. C.L., C.P., J.D. performed experiments. C.L., C.P., J.D., H.Y. analyzed the data. C.L., H.Y. wrote the manuscript.

References

1. Huffman JW, Dai D., Martin B.R., Compton D.R.: **Design, synthesis and pharmacology of cannabimimetic indoles**. *Bioorganic & Medicinal Chemistry Letters* 1994, **4**(4):563-566.
2. Wiley JL, Compton DR, Dai D, Lainton JA, Phillips M, Huffman JW, Martin BR: **Structure-activity relationships of indole- and pyrrole-derived cannabinoids**. *J Pharmacol Exp Ther* 1998, **285**(3):995-1004.
3. Schwartz MD, Trecki J, Edison LA, Steck AR, Arnold JK, Gerona RR: **A Common Source Outbreak of Severe Delirium Associated with Exposure to the Novel Synthetic Cannabinoid ADB-PINACA**. *J Emerg Med* 2015, **48**(5):573-580.
4. Zapata F, Matey JM, Montalvo G, García-Ruiz C: **Chemical classification of new psychoactive substances (NPS)**. *Microchemical Journal* 2021, **163**:105877.
5. Adams AJ, Banister SD, Irizarry L, Trecki J, Schwartz M, Gerona R: **"Zombie" Outbreak Caused by the Synthetic Cannabinoid AMB-FUBINACA in New York**. *N Engl J Med* 2017, **376**(3):235-242.
6. Zaurova M, Hoffman RS, Vlahov D, Manini AF: **Clinical Effects of Synthetic Cannabinoid Receptor Agonists Compared with Marijuana in Emergency Department Patients with Acute Drug Overdose**. *J Med Toxicol* 2016, **12**(4):335-340.
7. Ford BM, Tai S, Fantegrossi WE, Prather PL: **Synthetic Pot: Not Your Grandfather's Marijuana**. *Trends Pharmacol Sci* 2017, **38**(3):257-276.
8. Marsicano G, Lutz B: **Expression of the cannabinoid receptor CB1 in distinct neuronal subpopulations in the adult mouse forebrain**. *Eur J Neurosci* 1999, **11**(12):4213-4225.
9. Kano M, Ohno-Shosaku T, Maejima T: **Retrograde signaling at central synapses via endogenous cannabinoids**. *Mol Psychiatry* 2002, **7**(3):234-235.
10. Piomelli D: **The molecular logic of endocannabinoid signalling**. *Nat Rev Neurosci* 2003, **4**(11):873-884.
11. Ohno-Shosaku T, Tsubokawa H, Mizushima I, Yoneda N, Zimmer A, Kano M: **Presynaptic cannabinoid sensitivity is a major determinant of depolarization-induced retrograde suppression at hippocampal synapses**. *J Neurosci* 2002, **22**(10):3864-3872.
12. Ravinet Trillou C, Delgorge C, Menet C, Arnone M, Soubrié P: **CB1 cannabinoid receptor knockout in mice leads to leanness, resistance to diet-induced obesity and enhanced leptin sensitivity**. *Int J Obes Relat Metab Disord* 2004, **28**(4):640-648.
13. Mendizábal VE, Adler-Graschinsky E: **Cannabinoids as therapeutic agents in cardiovascular disease: a tale of passions and illusions**. *Br J Pharmacol* 2007, **151**(4):427-440.
14. Malinowska B, Baranowska-Kuczko M, Schlicker E: **Triphasic blood pressure responses to cannabinoids: do we understand the mechanism?** *Br J Pharmacol* 2012, **165**(7):2073-2088.
15. Jiang M, Bajpayee NS: **Molecular mechanisms of go signaling**. *Neurosignals* 2009, **17**(1):23-41.
16. Foerster K, Groner F, Matthes J, Koch WJ, Birnbaumer L, Herzig S: **Cardioprotection specific for the G protein Gi2 in chronic adrenergic**

signaling through beta 2-adrenoceptors. *Proc Natl Acad Sci U S A* 2003, **100**(24):14475-14480.
17. Cha HL, Choi JM, Oh HH, Bashyal N, Kim SS, Birnbaumer L, Suh-Kim H: **Deletion of the α subunit of the heterotrimeric Go protein impairs cerebellar cortical development in mice**. *Mol Brain* 2019, **12**(1):57.
18. Hultman R, Kumari U, Michel N, Casey PJ: **Gαz regulates BDNF-induction of axon growth in cortical neurons**. *Mol Cell Neurosci* 2014, **58**:53-61.
19. Banister SD, Longworth M, Kevin R, Sachdev S, Santiago M, Stuart J, Mack JB, Glass M, McGregor IS, Connor M *et al*: **Pharmacology of Valinate and tert-Leucinate Synthetic Cannabinoids 5F-AMBICA, 5F-AMB, 5F-ADB, AMB-FUBINACA, MDMB-FUBINACA, MDMB-CHMICA, and Their Analogues**. *ACS Chem Neurosci* 2016, **7**(9):1241-1254.
20. Banister SD, Moir M, Stuart J, Kevin RC, Wood KE, Longworth M, Wilkinson SM, Beinat C, Buchanan AS, Glass M *et al*: **Pharmacology of Indole and Indazole Synthetic Cannabinoid Designer Drugs AB-FUBINACA, ADB-FUBINACA, AB-PINACA, ADB-PINACA, 5F-AB-PINACA, 5F-ADB-PINACA, ADBICA, and 5F-ADBICA**. *ACS Chem Neurosci* 2015, **6**(9):1546-1559.
21. Finlay DB, Manning JJ, Ibsen MS, Macdonald CE, Patel M, Javitch JA, Banister SD, Glass M: **Do Toxic Synthetic Cannabinoid Receptor Agonists Have Signature in Vitro Activity Profiles? A Case Study of AMB-FUBINACA**. *ACS Chem Neurosci* 2019, **10**(10):4350-4360.
22. Patel M, Manning JJ, Finlay DB, Javitch JA, Banister SD, Grimsey NL, Glass M: **Signalling profiles of a structurally diverse panel of synthetic cannabinoid receptor agonists**. *Biochem Pharmacol* 2020, **175**:113871.
23. Ryalls B, Patel M, Sparkes E, Banister SD, Finlay DB, Glass M: **Investigating selectivity and bias for G protein subtypes and β-arrestins by synthetic cannabinoid receptor agonists at the cannabinoid CB1 receptor**. *Biochemical Pharmacology* 2024, **222**:116052.
24. Zagzoog A, Brandt AL, Black T, Kim ED, Burkart R, Patel M, Jin Z, Nikolaeva M, Laprairie RB: **Assessment of select synthetic cannabinoid receptor agonist bias and selectivity between the type 1 and type 2 cannabinoid receptor**. *Sci Rep* 2021, **11**(1):10611.
25. Schrage R, De Min A, Hochheiser K, Kostenis E, Mohr K: **Superagonism at G protein-coupled receptors and beyond**. *Br J Pharmacol* 2016, **173**(20):3018-3027.
26. Yano H, Chitsazi R, Lucaj C, Tran P, Hoffman AF, Baumann MH, Lupica CR, Shi L: **Subtle Structural Modification of a Synthetic Cannabinoid Receptor Agonist Drastically Increases its Efficacy at the CB1 Receptor**. *ACS Chemical Neuroscience* 2023, **14**(21):3928-3940.
27. Krishna Kumar K, Robertson MJ, Thadhani E, Wang H, Suomivuori CM, Powers AS, Ji L, Nikas SP, Dror RO, Inoue A *et al*: **Structural basis for activation of CB1 by an endocannabinoid analog**. *Nat Commun* 2023, **14**(1):2672.
28. Krishna Kumar K, Shalev-Benami M, Robertson MJ, Hu H, Banister SD, Hollingsworth SA, Latorraca NR, Kato HE, Hilger D, Maeda S *et al*: **Structure of a Signaling Cannabinoid Receptor 1-G Protein Complex**. *Cell* 2019, **176**(3):448-458.e412.

29. Brust CA, Swanson MA, Tsoutsouvas CI, Dimova ST, Dang VQ, Stahl EL, Ho J-H, Nikas SP, Makriyannis A, Bohn LM: **Comparison of Agonist Activity between CB1 and CB2 Receptors with Orthosteric Site Mutations**. *Receptors* 2024, **3**(3):380-396.
30. Semeano A, Garland R, Bonifazi A, Lee KH, Famiglietti J, Zhang W, Jo YJ, Battiti FO, Shi L, Newman AH *et al*: **Linkers in Bitopic Agonists Shape Bias Profile among Transducers for the Dopamine D2 and D3 Receptors**. *ACS Pharmacology & Translational Science* 2024, **7**(8):2333-2349.
31. Sánchez-Soto M, Bonifazi A, Cai NS, Ellenberger MP, Newman AH, Ferré S, Yano H: **Evidence for Noncanonical Neurotransmitter Activation: Norepinephrine as a Dopamine D₂-Like Receptor Agonist**. *Molecular Pharmacology* 2016, **89**(4):457-466.
32. Bonifazi A, Yano H, Guerrero AM, Kumar V, Hoffman AF, Lupica CR, Shi L, Newman AH: **Novel and Potent Dopamine D(2) Receptor Go-Protein Biased Agonists**. *ACS Pharmacol Transl Sci* 2019, **2**(1):52-65.
33. Usui K, Fujita Y, Kamijo Y, Kokaji T, Funayama M: **Identification of 5-fluoro ADB in human whole blood in four death cases**. *Journal of analytical toxicology* 2018, **42**(2):e21-e25.
34. Boland DM, Reidy LJ, Seither JM, Radtke JM, Lew EO: **Forty-three fatalities involving the synthetic cannabinoid, 5-fluoro-ADB: Forensic pathology and toxicology implications**. *Journal of forensic sciences* 2020, **65**(1):170-182.
35. Schrage R, Seemann WK, Klöckner J, Dallanoce C, Racké K, Kostenis E, De Amici M, Holzgrabe U, Mohr K: **Agonists with supraphysiological efficacy at the muscarinic M2 ACh receptor**. *Br J Pharmacol* 2013, **169**(2):357-370.
36. Cabanlong CV, Russell LN, Fantegrossi WE, Prather PL: **Metabolites of Synthetic Cannabinoid 5F-MDMB-PINACA Retain Affinity, Act as High Efficacy Agonists and Exhibit Atypical Pharmacodynamic Properties at CB1 Receptors**. *Toxicol Sci* 2022, **187**(1):175-185.
37. Banister SD, Connor M: **The Chemistry and Pharmacology of Synthetic Cannabinoid Receptor Agonists as New Psychoactive Substances: Origins**. *Handb Exp Pharmacol* 2018, **252**:165-190.
38. Daigle TL, Kwok ML, Mackie K: **Regulation of CB1 cannabinoid receptor internalization by a promiscuous phosphorylation-dependent mechanism**. *J Neurochem* 2008, **106**(1):70-82.
39. Jin W, Brown S, Roche JP, Hsieh C, Celver JP, Kovoor A, Chavkin C, Mackie K: **Distinct domains of the CB1 cannabinoid receptor mediate desensitization and internalization**. *J Neurosci* 1999, **19**(10):3773-3780.

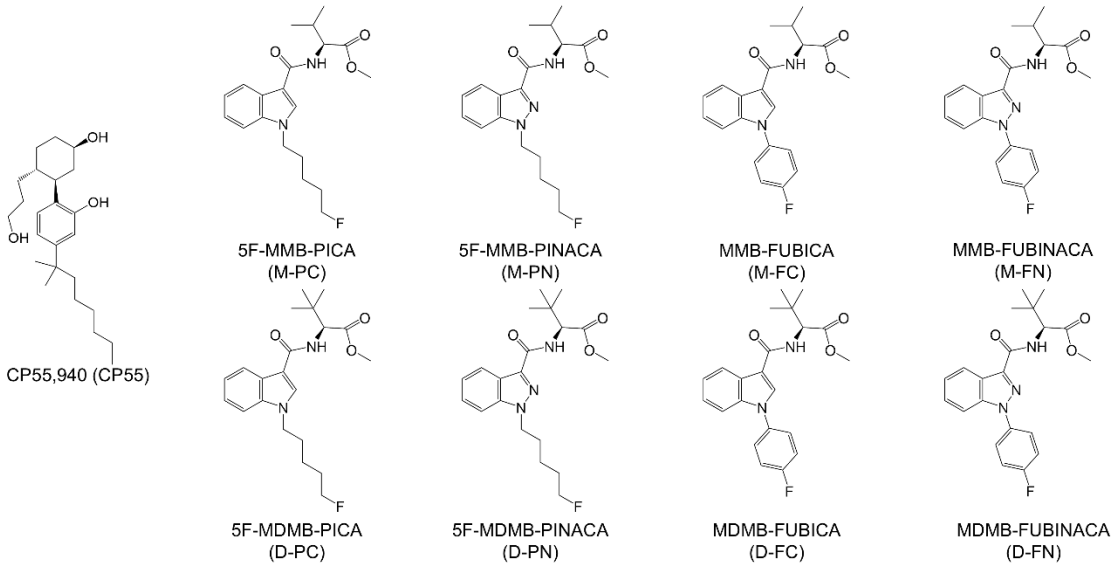

Figure 1: Structures of SCRAs used in this study. CP55,940 serves as the reference ligand for all experiments.

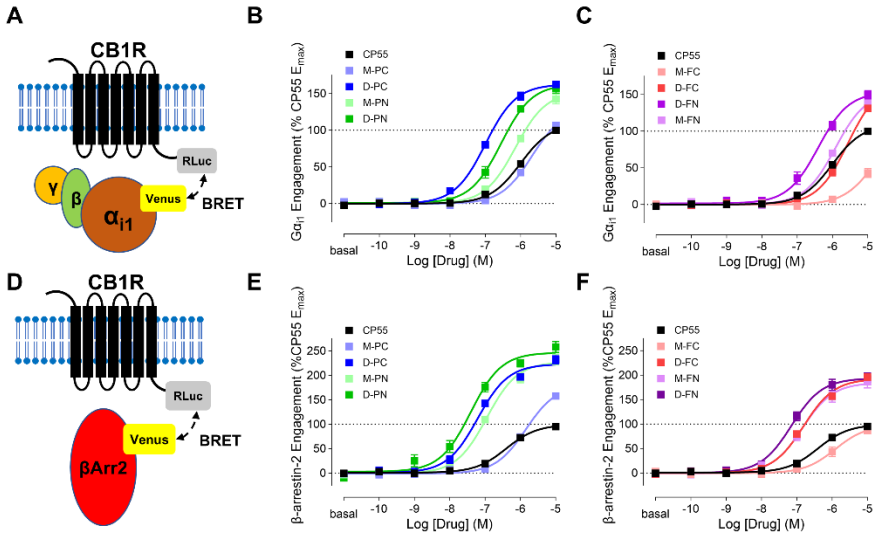

Figure 2: SCRA-induced $G\alpha_{i1}$ and β-Arr2 engagement to CB1R. Drug-induced BRET between CB1R-RLuc and $G\alpha_{i1}$-Venus (A-C) or β-Arr2-Venus (D-F) are shown. Concentration-response curves of SCRA-induced BRET are plotted as a percentage of CP55 E_{max} (B-C, $G\alpha_{i1}$; E-F, β-Arr2) and organized by tail moiety (B,E 5-fluoropentyl; C,F 4-fluorobenzyl). Data are presented as means ± SEM of n=4 experiments.

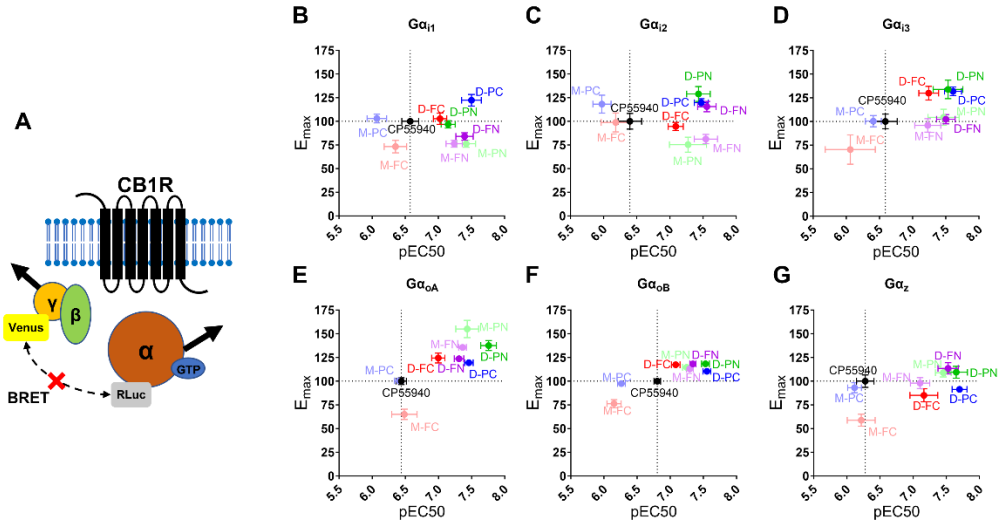

Figure 3: SCRA-activated $G\alpha_{i/o}$ subtype protein dissociation BRET assay. Cartoon illustrating BRET interaction between CB1R and Gα-RLuc and $G\gamma_2$-Venus with untagged CB1R (A). SCRA-induced BRET efficacy, as a percentage of CP55 E_{max}, and pEC50 were plotted for $G\alpha_{i/o}$ subtype transducers: $G\alpha_{i1}$ (B), $G\alpha_{i2}$ (C), $G\alpha_{i3}$ (D), $G\alpha_{oA}$ (E), $G\alpha_{oB}$ (F), and $G\alpha_z$ (G). Data presented as means ± SEM of n=4 experiments.

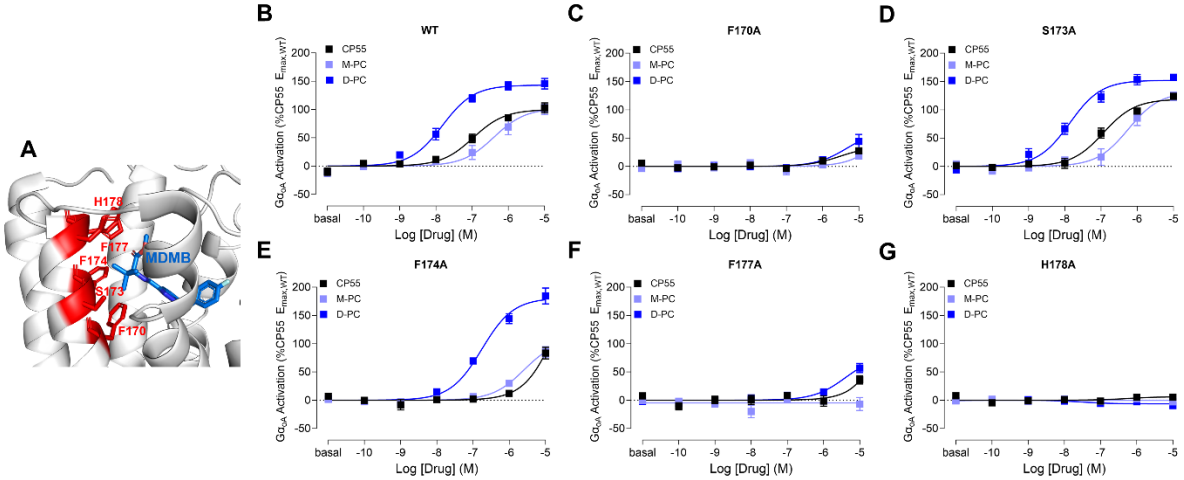

Figure 4: CB1R-TM2 mutational analysis of SCRA head moiety interaction. A close-up view of TM2-MDMB-FUBINACA (PDB:6N4B) with residues (red) within 4 Å of the MDMB-head moiety (blue) using PyMOL 3.0 (Schrödinger) for visualization (A). Through BRET $G\alpha_{oA}$ Activation mode, 5F-MMB-PICA and 5F-MDMB-PICA are compared to CP55 in the presence of CB1R with the following TM2 mutations: Wildtype (B), F170A (C), S173A (D), F174A (E), F177A (F), H178A (G). Concentration-response curves of SCRA-induced BRET plotted as a percentage of CP55 $E_{max,WT}$. Data presented as means ± SEM of n≥3 experiments.

Table 1: Pharmacological comparison of SCRAs in CB1R-transducer engagement BRET

	$G\alpha_{i1}$		βArr2		Bias Factor	
	E_{max} (% CP55)	pEC_{50} (M)	E_{max} (% CP55)	pEC_{50} (M)	ΔΔlog	$G\alpha_{i1}$ - βArr2
CP55	100 ± 1.14	6.00 ± 0.04	100 ± 4.72	6.37 ± 0.10		
M-PC	106.5 ± 4.40	5.69 ± 0.06	157.7 ± 5.21*	5.84 ± 0.05*	**M-PC - CP55**	-0.02
D-PC	162.3 ± 4.79*	7.00 ± 0.04*	231.7 ± 8.27*	7.21 ± 0.06*	**D-PC - CP55**	-0.01
M-PN	142.6 ± 6.63*	6.15 ± 0.05	232.3 ± 10.94*	6.95 ± 0.06*	**M-PN - CP55**	-0.64
D-PN	157.3 ± 6.97*	6.55 ± 0.06	258.0 ± 11.04*	7.40 ± 0.09*	**D-PN - CP55**	-0.68
M-FC	42.9 ± 6.03*	4.84 ± 0.56*	87.1 ± 7.33	5.91 ± 0.13*	**M-FC - CP55**	-1.15#
D-FC	131.0 ± 4.10*	5.56 ± 0.06	195.9 ± 6.92*	6.80 ± 0.05*	**D-FC - CP55**	-1.04#
M-FN	137.0 ± 4.94*	5.92 ± 0.05	185.9 ± 12.24*	6.84 ± 0.08*	**M-FN - CP55**	-0.69
D-FN	149.5 ± 5.67*	6.40 ± 0.08	192.0 ± 12.26*	7.15 ± 0.08*	**D-FN - CP55**	-0.49

Data analyzed by one-way ANOVA followed by post-hoc Dunnett test. Data presented as means ± SEM. Significance of * represents p>0.05 compared to CP55 E_{max} and pEC_{50} values for respective transducer. Bias factors greater than 1 or less than -1 are marked with #.

Table 2: Pharmacological comparison of SCRAs in G protein dissociation BRET

	$G\alpha_{i1}$		$G\alpha_{i2}$		$G\alpha_{i3}$		$G\alpha_{oA}$		$G\alpha_{oB}$		$G\alpha_{z}$	
	E_{max} (% CP55)	pEC_{50} (M)	E_{max} (% CP55)	pEC_{50} (M)	E_{max} (% CP55)	pEC_{50} (M)	E_{max} (% CP55)	pEC_{50} (M)	E_{max} (% CP55)	pEC_{50} (M)	E_{max} (% CP55)	pEC_{50} (M)
CP55	100 ± 3.13	6.58 ± 0.13	100 ± 8.22	6.4 ± 0.18	100 ± 7.81	6.59 ± 0.18	100 ± 3.62	6.44 ± 0.08	100 ± 2.10	6.81 ± 0.05	100 ± 6.55	6.28 ± 0.13
M-PC	102.9 ± 4.62	6.07 ± 0.08	118.2 ± 9.43	5.98 ± 0.14	100.3 ± 5.95	6.41 ± 0.13	100.4 ± 3.10	6.41 ± 0.07	97.4 ± 2.84	6.26 ± 0.06*	93.1 ± 5.27	6.12 ± 0.10
D-PC	122.3 ± 6.14*	7.5 ± 0.15*	119.6 ± 4.30	7.47 ± 0.10*	131.8 ± 4.53	7.61 ± 0.10*	119.4 ± 2.66	7.46 ± 0.07*	110.4 ± 2.21	7.55 ± 0.06*	91.4 ± 3.40	7.7 ± 0.11*
M-PN	74.7 ± 3.79*	7.42 ± 0.14*	75.3 ± 7.92	7.27 ± 0.28*	104.4 ± 8.50	7.47 ± 0.23*	155 ± 9.13*	7.43 ± 0.17*	114.6 ± 2.64*	7.25 ± 0.06*	108.9 ± 4.50	7.46 ± 0.12*
D-PN	96.9 ± 3.97	7.15 ± 0.11*	128.9 ± 7.91	7.43 ± 0.18*	133.8 ± 9.76	7.54 ± 0.22*	137.5 ± 5.24*	7.76 ± 0.12*	118.3 ± 2.35*	7.53 ± 0.06*	109.4 ± 6.21	7.65 ± 0.17*
M-FC	67.8 ± 6.65*	6.33 ± 0.20	99.6 ± 10.94	6.31 ± 0.26	68.3 ± 20.73	5.94 ± 0.49	64.6 ± 5.26*	6.85 ± 0.19	78.2 ± 4.70*	6.2 ± 0.11*	51.9 ± 6.50*	6.54 ± 0.28
D-FC	102.8 ± 4.28	7.03 ± 0.10	94.7 ± 4.33	7.09 ± 0.11	130.2 ± 7.27	7.24 ± 0.15	124.5 ± 5.15*	7 ± 0.10*	117.3 ± 3.04*	7.08 ± 0.06*	84.2 ± 6.95	7.16 ± 0.21*
M-FN	76.3 ± 3.57*	7.24 ± 0.12*	81.2 ± 4.85	7.54 ± 0.18*	95.8 ± 7.09	7.23 ± 0.20	135.6 ± 2.75*	7.36 ± 0.06*	112.9 ± 2.18*	7.29 ± 0.05*	97.9 ± 5.74	7.11 ± 0.15*
D-FN	84.1 ± 3.89	7.4 ± 0.13*	115.5 ± 5.49	7.56 ± 0.14*	102.3 ± 4.84	7.5 ± 0.14*	123.6 ± 3.21*	7.31 ± 0.07*	118.2 ± 1.98*	7.34 ± 0.05*	113.5 ± 5.94	7.53 ± 0.15*

Data analyzed by one-way ANOVA followed by post-hoc Dunnett test. Data presented as means ± SEM. Significance of * represents p>0.05 compared to CP55 E_{max} and pEC_{50} values for each respective transducer.

Table 3: SCRA-mediated activation bias of $G\alpha_{i/o}$ subtypes

ΔΔlog	$G\alpha_{i1}$ - $G\alpha_{i2}$	$G\alpha_{i1}$ - $G\alpha_{i3}$	$G\alpha_{i1}$ - $G\alpha_{oA}$	$G\alpha_{i1}$ - $G\alpha_{oB}$	$G\alpha_{i1}$ - $G\alpha_{z}$	$G\alpha_{i2}$ - $G\alpha_{i3}$	$G\alpha_{i2}$ - $G\alpha_{oA}$	$G\alpha_{i2}$ - $G\alpha_{oB}$	$G\alpha_{i2}$ - $G\alpha_{z}$	$G\alpha_{i3}$ - $G\alpha_{oA}$	$G\alpha_{i3}$ - $G\alpha_{oB}$	$G\alpha_{i3}$ - $G\alpha_{z}$	$G\alpha_{oA}$ - $G\alpha_{oB}$	$G\alpha_{oA}$ - $G\alpha_{z}$	$G\alpha_{oB}$ - $G\alpha_{z}$
M-PC - CP55	-0.15	-0.31	-0.46	0.06	-0.30	-0.17	-0.32	0.21	-0.16	-0.15	0.37	0.01	0.52	0.16	-0.36
D-PC - CP55	-0.14	-0.13	-0.09	0.22	-0.37	0.01	0.06	0.36	-0.23	0.04	0.35	-0.24	0.31	-0.29	-0.59
M-PN - CP55	0.40	-0.16	-0.02	0.25	-0.47	-0.55	-0.42	-0.15	-0.87	0.13	0.40	-0.31	0.27	-0.44	-0.71
D-PN - CP55	-0.24	-0.57	-0.54	-0.30	-0.91	-0.34	-0.30	-0.06	-0.67	0.04	0.28	-0.34	0.24	-0.37	-0.61
M-FC - CP55	-0.14	0.32	-0.22	0.41	-0.07	0.46	-0.08	0.55	0.07	-0.54	0.09	-0.39	0.63	0.15	-0.48
D-FC - CP55	-0.21	-0.31	-0.19	0.11	-0.35	-0.10	0.01	0.32	-0.15	0.11	0.42	-0.05	0.31	-0.16	-0.47
M-FN - CP55	-0.31	-0.29	-0.31	-0.20	-0.48	0.02	0.01	0.11	-0.17	-0.02	0.09	-0.19	0.10	-0.18	-0.28
D-FN - CP55	-0.28	-0.39	-0.01	-0.07	-0.77	-0.11	0.27	0.21	-0.49	0.38	0.32	-0.38	-0.06	-0.76	-0.70

Table 4: CB1R-TM2 Mutational Analysis with SCRA Head Moiety

	WT		F170A		S173A		F174A		F177A		H178A	
	E_{max} (% CP55)	pEC_{50} (M)	E_{max} (% CP55)	pEC_{50} (M)	E_{max} (% CP55)	pEC_{50} (M)	E_{max} (% CP55)	pEC_{50} (M)	E_{max} (% CP55)	pEC_{50} (M)	E_{max} (% CP55)	pEC_{50} (M)
CP55	100 ± 8.62	6.97 ± 0.12	27.4* ± 3.47	5.51* ± 0.43	123.7 ± 5.5	6.93 ± 0.11	83.2 ± 10.35	6.44* ± 0.08	35.9* ± 7.42	N.D.	5.20* ± 3.56	N.D.
M-PC	100.3 ± 8.95	6.4 ± 0.2	18.3* ± 4.46	N.D.	123.9 ± 7.28	6.25 ± 0.13	85.5 ± 9.01	6.41* ± 0.07	-6.90* ± 11.56	N.D.	-2.90* ± 5.21	N.D.
D-PC	145.5* ± 9.25	7.82 ± 0.1	44.0* ± 12.39	7.47* ± 0.1	157.3* ± 6.13	7.87 ± 0.1	184.5* ± 14.06	7.46 ± 0.07	57.0* ± 8.12	7.55* ± 0.06	-9.40* ± 3.62	N.D.

Data analyzed by one-way ANOVA followed by post-hoc Dunnett test. Data presented as means ± SEM. Significance of * represents p>0.05 compared to CP55 E_{max} of the wildtype construct. For concentration-response curves with an E_{max} less than 20% or with a poor-fit were not determined (N.D.)